Journal of Mathematical Chemistry 14 (1993) 7–20

Lattice models for the collapse of branched polymers

S. Flesia

Department of Physics, King's College London, London WC2R 2LS, UK

Randomly branched polymers in dilute solution in a good solvent can be modelled by lattice animals (i.e. connected clusters). Introducing attractive monomer–monomer interactions between nearest-neighbour sites causes the branched polymer to become more compact and a collapse transition, analogous to that in linear polymers, is expected to occur at low temperature. This model, and alternative lattice models for the collapse transition of branched polymers, will be described. In each of the models, the collapse is driven by some kind of near-neighbour fugacity, cycle fugacity or perimeter fugacity. In two and three dimensions and on several lattices, analytical results for the free energy and numerical results, using exact enumeration data, for the free energy and for the specific heat, will be presented with estimates of the cross-over exponent ϕ and the collapse temperature T_c.

1. Introduction

Just as linear polymers in dilute solution can be modelled by self-avoiding walks on lattices, randomly branched polymers in dilute solution can be modelled by lattice animals. In this system (one polymer in a solvent) there are two main interactions: monomer–solvent (ϵ_1) and monomer–monomer (ϵ_2) interaction. The temperature parameter can be written as $\beta = \epsilon/kT$, where k is the Boltzmann constant and $\epsilon_1(\epsilon_2)$ is the interaction parameter. Intuitively $\epsilon_1(\epsilon_2)$ describes the quality of the solvent. In a "good solvent" the polymer–solvent attractive interactions are highly favoured, $\epsilon_1 \gg 0$, hence the polymer is an extended random animal (swollen phase). In a "poor solvent" the attractive interactions between monomers are highly favoured, $\epsilon_2 \gg 0$, and the polymer shrinks to a compact globule state when the temperature is lowered below a critical temperature T_c (compact or collapsed phase). It is believed that at temperature T_c the polymer undergoes a collapse transition similar to that of linear polymers [1–4]. Although for branched polymers the existence of this transition is not proved, there is substantial numerical evidence for its existence [5–13]. Another interesting case that can be treated, is when the interaction between monomers and solvent is strong and repulsive, $\epsilon_1 < 0$, such that the polymer is forced to a compact phase by the repulsive action of the solvent. Nevertheless, the aim of this paper is only to discuss a number of related, one-variable, lattice models in which the collapse is driven by some kind of nearest-neighbour or cycle or perimeter fugacity and to point out the relations between the

models. The models have been studied on trees [12], lattice animals [13] and c-animals [14], on several lattices in both two and three dimensions with the aid of new exact enumeration data. A generalised two variables model including all these interactions has been recently studied [15].

2. Models of branched polymers

Let us recall some definitions and terminology.

An example of a lattice animal on the square lattice is shown in fig. 1. It has: eight sites (N), eight bonds (B), one cycle (C), two pairs of nearest-neighbour sites not directly connected by a bond, i.e. contacts (K), ten pairs of nearest-neighbour sites (P)($P = B + K$), fourteen *bond percolation perimeter* bonds (Q) and twelve *solvent perimeter* bonds (S), i.e. pairs of bonds which join an occupied site to a nearest-neighbour site which is unoccupied ($S = Q - K$). There exist three relations connecting these quantities,

$$C = B - N + 1 \qquad \text{Euler's relation}, \tag{2.1}$$

$$Q = ZN - 2B - K \qquad \text{Bond percolation perimeter}, \tag{2.2}$$

$$S = ZN - 2B - 2K \qquad \text{Bond solvent perimeter}, \tag{2.3}$$

where z is the coordination number. For a hypercubic lattice $Z = 2d$ (d is the dimension of the system). An animal may be weakly embedded or strongly embedded (in this case $K = 0$) in the lattice and the size of an animal may be measured either by its site content, N, or its bond content, B. If the number of cycles is zero ($C = 0$) it is called a *tree*, and if it has a prescribed number, C, of cycles it is called a *c-animal*.

Six underlying models are identified depending on whether the animals are weighted by $e^{\beta C}, e^{\beta K}, e^{\beta B}, e^{\beta P}, e^{\beta S}, e^{\beta Q}$, where β is proportional to the inverse temperature and e^{β} is the appropriate fugacity; the model weighted by $e^{\beta Q}$ is not considered in this paper (see ref. [15]). Each model has four different realizations (strongly or weakly embedded, site or bond counting). The resulting twenty models can be denoted by lower case letters (c-, k-, b-, p-, s-) when the animals are weakly embedded in the lattice and by upper case letters C-, K-, B-, P-, S-) when they are strongly embedded. A letter is primed when size is being measured by bond content.

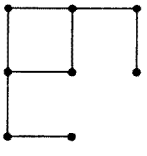

Fig. 1. Animal on the square lattice.

Let w be a generic name for the model, ($w = K, k, C, \ldots$) and u a generic name for the size content ($u = N, B$). The canonical partition function of the w-model is then:

$$Z_u(\beta, w) = \sum_w a(u, w) e^{\beta w}, \tag{2.4}$$

where $a(u, w)$ is the number of weakly or strongly embedded animals with u sites or bonds, and w contacts or cycles or perimeter or ....

Fortunately, several of those models can be proved to be equivalent. Five of the above models are trivial in the sense that the specific heat is identically zero. They are: the K-model and the K'-model, because $K = 0$ for strongly embedded animals, so the partition function is a constant and consequently the specific heat is zero; the b'-model, in fact, because of the bond counting, the fugacity per bond is a constant which can be taken off the sum, consequently the limiting free energy is a constant independent of β so that the specific heat is zero; finally, the P'-model and the B'-model are identical because they differ only by K which is zero for strongly embedded animals, and they are trivial for the same reason as the b'-model. Some of the other models are equivalent: the P-model and the B-model are identical because $P = B$ for strongly embedded animals, and they are both equivalent to the C-model; in fact from the relation (2.1) the partition function of the B-model can be written as

$$Z_N(\beta, B) = \sum_B a(N, B) e^{\beta B} = e^{\beta(N-1)} \sum_C a(N, C) e^{\beta C} = e^{\beta(N-1)} Z_N(\beta, C), \tag{2.5}$$

where $Z_N(\beta, C)$ is the partition function of the C-model, so they have the same specific heat. Using the same argument it is easy to prove that the b-model is equivalent to the c-model. Finally the p'-model is equivalent to the k'-model. Hence there are eleven independent non-trivial models, which may be taken to be

$$C, C', c, c', k, k', p, S, S', s, s'. \tag{2.6}$$

The p-model will not be considered in this paper. So there are the three main kinds of lattice model depending on whether the collapse is driven by some kind of near-neighbour contacts (K) or cycle (C) or bond solvent perimeter fugacity (S).

The models [11] are being studied for animals, c-animals and trees, on several lattices in both two and three dimensions with the aid of new exact enumeration data. The only models studied by other workers are the C-model and the c'-model. In fact Derrida and Herrmann [5] studied, with the transfer matrix method, the P-model which is equivalent to the C-model, Dickman and Schieve [6,7] and Lam [8,9] studied, with the Monte Carlo method, the B-model which is also equivalent to the C-model, Chang and Shapir [10] studied the C-model and the c'-model.

In the contact model only an attractive ($\epsilon_2 > 0$) monomer–monomer interaction between nearest-neighbour contacts is introduced to induce the collapse of the lattice animal at low temperature. Intuitively, an attractive interaction between monomers causes a swollen polymer to contract into a compact structure as the

number of contacts is increased. In this model, of course, only weakly embedded animals can be considered.

In the cycle model the collapse is driven by an increasing number of cycles (cycle fugacity) and, hence is only relevant to an animal model. This model seems less appropriate than the contact model to describe the collapse transition in polymers. Lubensky and Isaacson [16] suggested that cycles are relatively unimportant in determining the universality class and the number of cycles is not a relevant parameter; Knezević and Vannimenus [17] showed that the existence of loops are irrelevant as far as large-scale properties are concerned and several other numerical studies have supported this proposal [18]. This has led to trees being considered as useful model of branched polymers. However, it is also a good model of collapsing branched polymers and we will show in sections 4.2 and 4.3 that for a collapsing branched polymer with contact or bond solvent fugacities, trees are in the same universality class.

The solvent model describes the interaction between polymer and solvent. This time the collapse is driven by the repulsive action of the solvent on the polymer. The polymer is modelled by an animal or tree, the solvent by the unoccupied lattice sites, and the repulsive action on the polymer by the solvent is represented by the solvent perimeter bonds. We will see later that this model is related to the other two.

3. Contact model in trees

3.1. FREE ENERGY

This model has been studied by Gaunt and Flesia [12], so only a short description will be presented. It must be stressed that since the number of sites (N) and the number of bonds (B) are trivially related by the relation (2.1); in the case of trees and c-animals, it is irrelevant whether the size of the tree is classified by its site or its bond content. So, the canonical partition function of the k-model in trees is

$$Z_N(\beta, k) = \sum_K a(N, K) e^{\beta K}, \tag{3.1}$$

where $a(N, K)$ is the number of weakly embedded trees with N sites and K contacts. $\beta \geqslant 0$ corresponds to an attractive interaction ($\epsilon_2 > 0$) and $\beta \leqslant 0$ to a repulsive interaction ($\epsilon_2 < 0$). The reduced free energy is defined by

$$F_N(\beta) = N^{-1} \log Z_N(\beta) \tag{3.2}$$

and the limiting reduced free energy by

$$F(\beta) = \lim_{N \to \infty} F_N(\beta). \tag{3.3}$$

For a d-dimensional hypercubic lattice, Madras et al. [19] proved a number of rigorous results relating to $F(\beta)$. In particular they proved that the limiting free

energy (3.3) exists for $-\infty \leqslant \beta < \infty$ and they showed that this function is convex, monotone, non-decreasing and continuous for $-\infty < \beta < \infty$. If Λ_0 and λ_0 are the growth constants for strong and weak embeddings, respectively, then

$$F(-\infty) = \log \Lambda_0 \tag{3.4}$$

and

$$F(0) = \log \lambda_0 , \tag{3.5}$$

although there is no proof that $\lim_{\beta \to -\infty} F(\beta) = \log \Lambda_0$. So $\log \Lambda_0$ and $\log \lambda_0$ are, respectively, the lower and upper bounds for $\beta < 0$. Furthermore, Madras et al. [19] derived for $\beta > 0$ the following upper and lower bounds:

$$(d-1)\beta \leqslant F(\beta) \leqslant F(0) + (d-1)\beta , \tag{3.6}$$

where d is the dimension. Dividing by β and letting β go to infinity, gives

$$\lim_{\beta \to \infty} F(\beta)/\beta = d - 1 \tag{3.7}$$

and, moreover, there is an asymptotic line

$$L(\beta) = (d-1)\beta + S \tag{3.8}$$

such that $\lim_{\beta \to \infty}[F(\beta) - L(\beta)] = 0$. Physically S is interpreted as the reduced limiting entropy of the compact phase. A knowledge of the reduced limiting entropy and the dimension of the system gives the asymptotic behaviour of the reduced free energy. In fact it can be proved that

$$\pi^{-d} \int_0^{\pi} \dots \int_0^{\pi} \log\left(2d - 2\sum_{i=1}^{d} \cos \alpha_i\right) \mathrm{d}\alpha_1 \dots \mathrm{d}\alpha_d \leqslant S \leqslant d \log d - (d-1)\log(d-1) . \tag{3.9}$$

So, in particular, for the square lattice ($d = 2$)

$$(4C/\pi =)\ 1.1666\ldots \leqslant S \leqslant 1.386\ldots , \tag{3.10}$$

where C is Catalan's constant, and for the simple cubic lattice ($d = 3$)

$$1.673\ldots \leqslant S \leqslant 1.909 . \tag{3.11}$$

Because of the convexity of the limiting reduced free energy, the lower bounds (3.10) (in $d = 2$) and (3.11) (in $d = 3$) of the asymptote are in fact the improved lower bounds for $F(\beta)$ and the estimates of $[F(\beta) - (d-1)\beta]$ for increasing value of $\beta > 0$ (see ref. [12]) suggest that S is close or equal to the lower bounds in (3.10) and (3.11), respectively.

Numerical results

This paragraph reviews the numerical results of the β dependence of the limiting free energy in two dimensions (square lattice). For more details and for the three-

dimensional case one should refer to ref. [12]. These estimates are based on the exact enumeration data derived by Sykes [19–23] and Martin [24] using the *shadow method* [25]. From these data, the partition function and consequently, the reduced free energy are computed for all $N \leqslant 19$. Finally, the limiting reduced free energy $F(\beta)$ is estimated using the ratio method and the Padé approximant method, and then compared with the analytical results described in the first part of this section. Using the data above-mentioned, the reduced free energy $F_N(\beta)$, defined in eq. (3.2), is calculated for all $N \leqslant 19$. The results are plotted in fig. 2 where the dotted lines are the analytical bounds (3.4), (3.5), (3.6) and (3.8) given above, and the numerical estimates used [26] are: $\log \Lambda_0 = 1.334 \pm 0.002$, $\log \lambda_0 = 1.637 \pm 0.002$. The reduced limiting free energy is the limit of these curves and must lie somewhere between the rigorous lower and upper bounds. From fig. 2 it is easy to see that these curves are still outside the bounds hence considerable extrapolation is required to estimate $F(\beta)$, especially for large β. The curves are almost constants and easier to extrapolate for negative β, while, for increasing positive β, the curves spread out. The estimates of the limiting reduced free energy on the square lattice are tabulated in table 1. The estimation methods which have been used (ratio and Padé) give satisfactory and consistent estimates of the $F(\beta)$ for $\beta < 0$ and for small positive β. However, both methods rapidly become less precise for larger values of β, and for $\beta \geqslant 1.5$ they fail to provide estimates of any reliability. In section 4 a method to improve these estimates for large β will be presented.

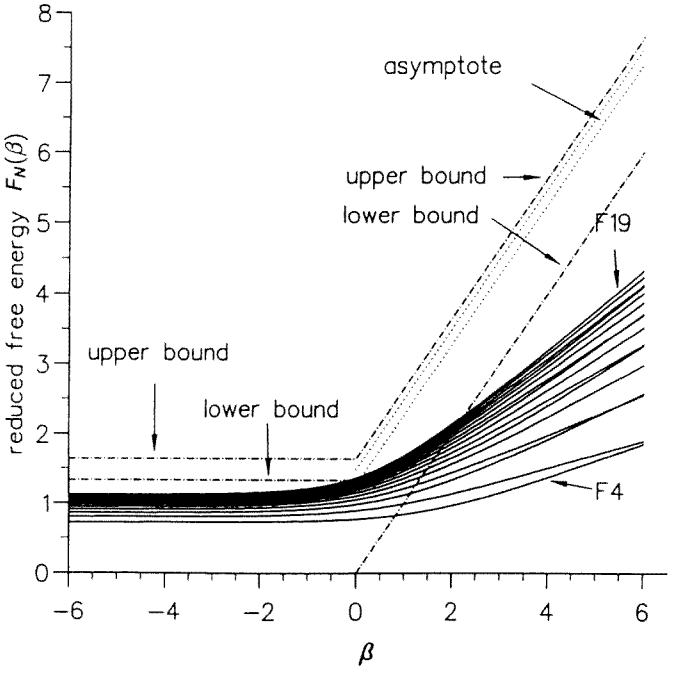

Fig. 2. The reduced free energy, $F_N(\beta)$, of the contact model for trees on the square lattice for $N = 4$–19. Upper and lower bounds to $F(\beta)$ and the asymptotic line $L(\beta)$, are included.

Table 1
Estimates of the limiting free energy on square lattice trees.

β	Contact model		Solvent model
	direct estimates	indirect estimates	direct estimates
−4.0	1.339 ± 0.002	1.339 ± 0.001	
−3.5	1.342 ± 0.002	1.342 ± 0.001	
−3.0	1.348 ± 0.002	1.347 ± 0.001	
−2.5	1.356 ± 0.002	1.356 ± 0.001	
−2.0	1.371 ± 0.001	1.371 ± 0.001	
−1.5	1.396 ± 0.001	1.396 ± 0.001	0.7 ± 0.2
−1.0	1.439 ± 0.002	1.439 ± 0.001	1.0 ± 0.2
−0.5	1.513 ± 0.001	1.513 ± 0.001	1.20 ± 0.04
0	1.637 ± 0.002	1.638 ± 0.002	1.637 ± 0.002
0.1	1.669 ± 0.002	1.670 ± 0.001	1.779 ± 0.001
0.2	1.707 ± 0.002	1.707 ± 0.001	1.932 ± 0.001
0.3	1.749 ± 0.002	1.749 ± 0.001	2.094 ± 0.001
0.4	1.797 ± 0.003	1.797 ± 0.002	2.264 ± 0.001
0.5	1.850 ± 0.005	1.851 ± 0.002	2.439 ± 0.001
0.6	1.906 ± 0.006	1.909 ± 0.003	2.619 ± 0.001
0.7	1.969 ± 0.007	1.971 ± 0.004	2.803 ± 0.001
0.8	2.032 ± 0.009	2.036 ± 0.005	2.990 ± 0.001
0.9	2.10 ± 0.02	2.12 ± 0.01	3.179 ± 0.001
1.0	2.16 ± 0.04	2.20 ± 0.04	3.371 ± 0.001
1.1	2.23 ± 0.04	2.27 ± 0.04	3.564 ± 0.001
1.2	2.29 ± 0.07	2.35 ± 0.04	3.758 ± 0.001
1.3	2.36 ± 0.10	2.43 ± 0.07	3.954 ± 0.001
1.4	2.44 ± 0.15	2.46 ± 0.09	4.150 ± 0.001
1.5	2.50 ± 0.20	2.55 ± 0.1	4.347 ± 0.001
1.6		2.62 ± 0.1	4.547 ± 0.001
1.7		2.73 ± 0.2	4.745 ± 0.001
1.8		2.82 ± 0.2	4.942 ± 0.001
1.9		2.88 ± 0.2	5.141 ± 0.001
2.0		3.0 ± 0.2	5.339 ± 0.001
2.1		3.09 ± 0.2	5.545 ± 0.001
2.2		3.16 ± 0.2	5.749 ± 0.001
2.3		3.20 ± 0.2	5.954 ± 0.001
2.4		3.30 ± 0.2	6.157 ± 0.001
2.5		3.46 ± 0.2	6.334 ± 0.001
3.0		3.7 ± 0.3	7.334 ± 0.001
3.5			8.334 ± 0.001
4.0			9.334 ± 0.001

3.2. SPECIFIC HEAT AND CROSSOVER EXPONENT

As can be seen in ref. [12] the limiting reduced free energy is very smooth and there is no indication of the collapse transition. $F(\beta)$ is expected to be analytic for $\beta \leqslant 0$ and the collapse is believed to occur at some value of $\beta = \beta_c > 0$. In fact, because of the attractive interaction ϵ_2, β must be positive or zero. Unfortunately

there are no analytic results about the specific heat; the rigorous results for $F(\beta)$ do not give any proof of a collapse transition or information about the behaviour of the second derivative. Therefore, in order to investigate the possibility of a collapse transition, the specific heat has been studied numerically.

The specific heat has been calculated following the definition of Chang and Shapir [10],

$$H_N = \frac{d^2 F_N(\beta)}{d\beta^2} = (\langle k^2 \rangle - \langle k \rangle^2)/N . \tag{3.12}$$

All the curves are dominated by a single sharp peak which increases smoothly and regularly in height as N increases [12]. Presumably this peak corresponds to the collapse transition. According to the finite size scaling theory [10], the height h_N of the Nth peak should scale as

$$h_N \sim N^{\alpha_0 \phi_0} \quad N \to \infty , \tag{3.13}$$

where α_0 is the specific heat exponent and ϕ_0 is the cross-over exponent. $\alpha_0 \phi_0$ can be estimated by calculating

$$\alpha_{0,N} \phi_{0,N} = \frac{\log(h_N / h_{N-1})}{\log[N/(N-1)]} , \tag{3.14}$$

which should approach $\alpha_0 \phi_0$ as $N \to \infty$. Using the hyperscaling relation,

$$\alpha_0 = 2 - 1/\phi_0 , \tag{3.15}$$

ϕ_0 can be estimated by calculating

$$\phi_{0,N} = \frac{1}{2} \left(\frac{\log(h_N / h_{N-1})}{\log[N/(N-1)]} \right), \tag{3.16}$$

which should approach ϕ_0 as $N \to \infty$. Estimates of $\phi_{0,N}$, together with the extrapolants, are plotted in ref. [12] as a function of $1/N$. The best estimate for the square lattice is

$$\phi_0 = 0.60 \pm 0.03 \quad (d = 2) . \tag{3.17}$$

In three dimensions the specific heat has been studied on the simple cubic (sc), body centred cubic (bcc) and diamond (diam) lattices. The best estimate is

$$\phi_0 = 0.82 \pm 0.03 \quad (d = 3) \tag{3.18}$$

for the bcc lattice, though it is consistent with less well-converged results for the sc and diam lattice.

Using finite size scaling theory, the critical temperature in two and three dimensions has been estimated in ref. [12].

4. Solvent model

In the solvent model the collapse is driven by the repulsive action of the solvent

on the polymer. The polymer is modelled by an animal or a c-animal or a tree, the solvent by the vacant lattice sites and the repulsive action on the polymer by the solvent is represented by the solvent perimeter bonds (2.3). As explained in section 2, four different representations of the perimeter model exist; they are the S, S', s, s'.

4.1. FREE ENERGY

In this section we discuss some properties of the free energy for the solvent model. In order to compare this section to section 3 we will restrict the discussion to the solvent model on weakly embedded trees, but the following proofs apply, mutatis mutandis, to the other models. The partition function of the s-model is

$$Z_N(\beta, s) = \sum_{C,K} a(N, C, K) e^{(zN-2C-2N+2-2K)\beta}, \tag{4.1}$$

where $a(N, C, K)$ is the number of weak embedding trees with N sites, C cycles and K contacts and the limiting reduced free energy is

$$F(\beta) = \lim_{N\to\infty} N^{-1} \log Z_N(\beta). \tag{4.2}$$

Using concatenation arguments similar to those in ref. [19], Flesia et al. [15] have proved that:

LEMMA 1

The $\lim_{N\to\infty} N^{-1} \log Z_N(\beta) = F(\beta)$ exists for $-\infty \leqslant \beta < \infty$ and $F(\beta)$ is monotone, non-decreasing, convex and continuous for $-\infty < \beta < \infty$.

And, if λ_0 is the growth constant for the weak embedding trees, then

$$F(0) = \log \lambda_0, \tag{4.3}$$

$$F(-\infty) = 0. \tag{4.4}$$

Flesia et al. [15] also proved that:

LEMMA 2

For $\beta > 0$

$$\log \Lambda_0 + 2(d-1)\beta \leqslant F(\beta) \leqslant F(0) + 2(d-1)\beta \tag{4.5}$$

and

$$\lim_{\beta\to\infty} F(\beta)/\beta = 2(d-1), \tag{4.6}$$

where Λ_0 is the growth constant for the strong embedding trees.

LEMMA 3

For $\beta < 0$

$$0 \leqslant F(\beta) \leqslant \log \lambda_0. \tag{4.7}$$

Numerical results

Because of the equivalence between bond and site counting for a tree model, only the later model has been studied.

Let us consider the square lattice. The reduced free energy on trees on the square lattice is calculated using the data of Sykes and Martin published in ref. [19] and it is plotted in fig. 3. In this graph for $\beta > 0$ the curves are nearly straight-lines with slope ~ 2 and the values of $F_N(\beta)$ decrease with increasing N. On the other hand, for $\beta < 0$, they are more spread out and the values of $F_N(\beta)$ increase with increasing N. At $\beta \approx 1$ they all cross. It should be noticed that, apart from the crossing point at $\beta \approx 1$, this graph seems to be closely similar in shape to the one for the contact-model. The numerical estimates of the limiting reduced free energy on the square lattice are given in table 1. The relation between the two models is pointed out in the section 4.2.

4.2. RELATION BETWEEN SOLVENT MODEL AND CONTACT MODEL

Flesia et al. [15] proved the following theorem:

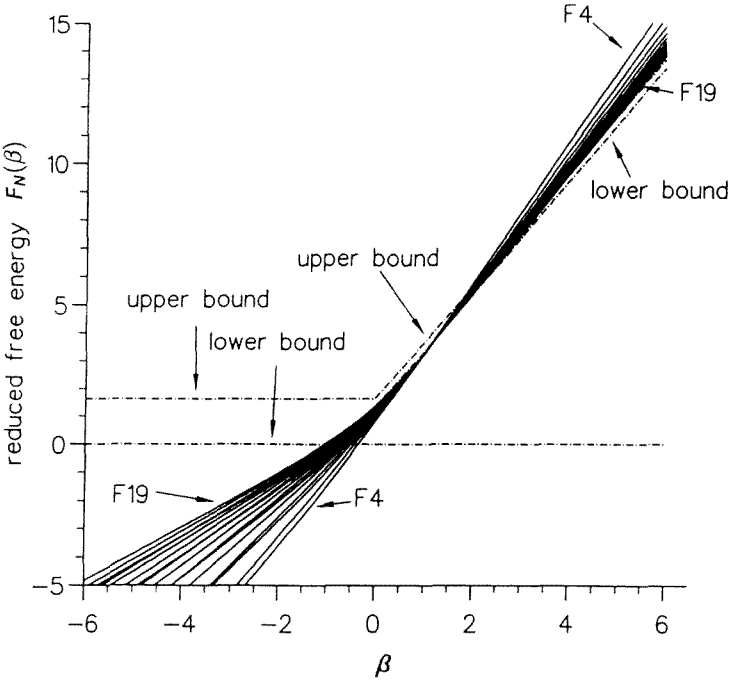

Fig. 3. The reduced free energy, $F_N(\beta)$, of the solvent model for trees on the square lattice for $N = 4$–19. Upper and lower bounds to $F(\beta)$ are included.

THEOREM 1

The limiting reduced free energy of the solvent model weak embedding in c-animals is related to the limiting reduced free energy of the contact model in c-animals by the following relation:

$$F^{c}(\beta,k) = (d-1)\beta + F^{c}(-\tfrac{1}{2}\beta,s)\,, \tag{4.8}$$

where $F^{c}(\beta,k)$ is the limiting reduced free energy for the contact model in c-animals and $F^{c}(-\frac{1}{2}\beta,s)$ is the limiting reduced free energy for the solvent model in c-animals.

We point out that since

$$F^{c}(\beta,k) = F^{0}(\beta,k) \tag{4.9}$$

[14], it follows using (4.8) and (4.9) that

$$F^{c}(\beta,s) = F^{0}(\beta,s)\,, \tag{4.10}$$

where $F^{0}(\beta,k)$ and $F^{0}(\beta,s)$ are, respectively, the limiting reduced free energy for the contact model in trees and for the solvent model in trees.

Theorem 1 is useful not only to clarify the relations existing between the models, but also to improve the estimates of the free energy. In fact the solvent model can be useful to estimate the behaviour of the limiting reduced free energy of the contact model at large positive β, and vice versa. For example: $F^{0}(\beta=2,k)$ for the contact model in trees in two dimensions, has no reliable estimation, but this corresponds, in the solvent model, to $F^{0}(\beta=-1,s)$ for which a reasonable estimate is available: $F^{0}(\beta=-1,s) = 1.0 \pm 0.2$. This gives for the contact model the value $F^{0}(\beta=2,k) = 3.0 \pm 0.2$ which is inside the analytic bounds.

In table 1 are tabulated the direct estimates of the limiting reduced free energy for the solvent model and the contact model in trees on the square lattice and the indirect estimates of the contact model in trees derived from relation (4.8). However, for ease of presentation, not all the estimates of the free energy of the solvent model used to calculate the indirect estimates of the free energy of the contact model are included in table 1. The direct and indirect estimates are in very good agreement. It should be noticed that for values of $\beta \geqslant 2.5$ for the solvent model, the asymptotic region is already reached. In fact using the relation (4.8), the corresponding value in the contact model, 1.334, is the lower bound $\log \Lambda_0$.

A similar analysis applies in three dimensions for the simple cubic lattice.

4.3. SPECIFIC HEAT AND CROSSOVER EXPONENT

The specific heat for the square lattice is plotted in fig. 4; the curves for different N have the same shape, but different size than those for the contact model, and this time, as expected, the peaks appear for negative values of β. The critical temperature of the solvent model for trees is related to the critical temperature of the

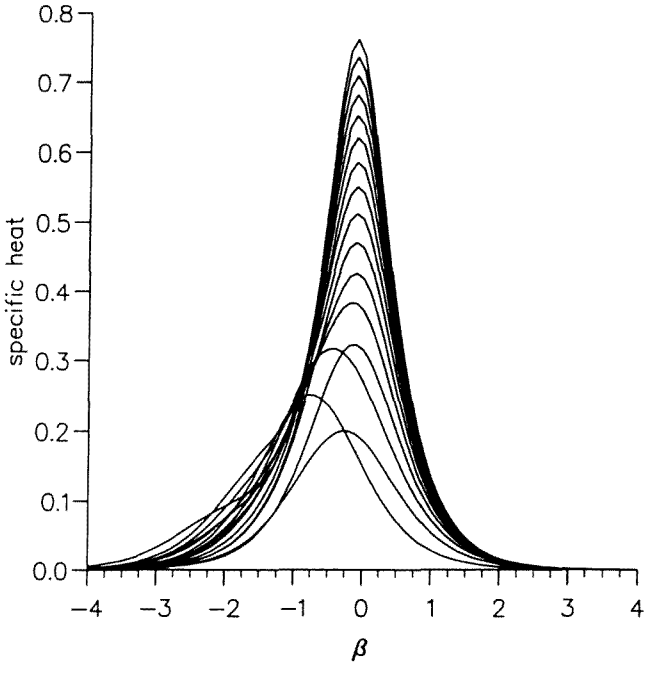

Fig. 4. The specific heat, $H_N(\beta)$, for the solvent model in trees on the square lattice for $N = 4$–19.

contact model for trees by the relation (4.8). Moreover, because of this relation and the hyperscaling relation, the crossover exponent ϕ is the same in the two models.

4.4. RELATION BETWEEN SOLVENT MODEL AND CYCLE-MODEL

Similarly to theorem 1, Flesia et al. [15] proved the following theorems:

THEOREM 2

The limiting reduced free energy of the solvent model in animals strong embeddings site counting is related to the limiting reduced free energy for the cycle-model animal strong embeddings site counting by the following relation:

$$F(\beta, C) = (d-1)\beta + F(-\tfrac{1}{2}\beta, S)\,. \tag{4.11}$$

THEOREM 3

The limiting reduced free energy of the solvent model in animals strong embeddings and bond counting is related to the limiting reduced free energy for the cycle-model animals strong embeddings and bond counting by the following relation:

Table 2
Summary of the models.

Animals	c-animals	Trees
C, C', c, c'		
k, k'	k	k
S, S', s, s'	s, s'	s, s'

$$F(\beta, C') = \frac{(d-1)}{d}\beta + F\left(-\frac{\beta}{2d}, S'\right). \tag{4.12}$$

The same comments as for theorem 1 about improving numerical estimates can be made again here and, in the case of the bond counting model, the estimates are even better because now β is related to $-\beta/2d$ instead of $-\beta/2$ and so they also improve with dimensionality.

5. Summary and conclusion

In this paper the collapse transition of branched polymers has been investigated. Several lattice models have been presented in section 2 and two of those models have been described in more detail in sections 3 and 4. Relations between models have been demonstrated analytically and numerically investigated in section 4.2. These relations have also been used to improve the numerical estimates of the limiting free energy and to find the critical temperature and the crossover exponent (sections 4.2 and 4.3). A summary of the models is presented in table 2.

Acknowledgement

The author appreciates helpful conversations with D.S. Gaunt, S.G. Whittington, C.E. Soteros, and M.F. Sykes. This research was financially supported, in part, by the SERC (grant number GR/G 05834).

References

[1] J. Mazur and F.L. McCrackin, J. Chem. Phys. 49 (1968) 648.
[2] R. Finsy, M. Janssens and A. Bellemans, J. Phys. A 8 (1975) L106.
[3] H.J. Saleur, J. Stat. Phys. 45 (1986) 419.
[4] H. Meirovitch and H.A. Lim, Phys. Rev. A 39 (1989) 4186.
[5] B. Derrida and H.J. Herrmann, J. Phys. (Paris) 44 (1983) 1365.
[6] R. Dickman and W.C. Shieve, J. Phys. (Paris) 45 (1984) 1727.
[7] R. Dickman and W.C. Shieve, J. Stat. Phys. 44 (1986) 465.
[8] P.M. Lam, Phys. Rev. B 35 (1987) 6988.

[9] P.M. Lam, Phys. Rev. B 38 (1988) 2813.
[10] I.S. Chang and Y. Shapir, Phys. Rev. B38 (1988) 6736.
[11] D.S. Gaunt and S. Flesia, Physica A168 (1990) 602.
[12] D.S. Gaunt and S. Flesia, J. Phys. A 24 (1991) 3655.
[13] S. Flesia and D.S. Gaunt, J. Phys. A 25 (1992) 2127.
[14] S. Flesia, D.S. Gaunt, C.E. Soteros and S.G. Whittington, J. Phys. A 25 (1992) 3515.
[15] S. Flesia, D.S. Gaunt, C.E. Soteros and S.G. Whittington, J. Phys. A 25 (1992) L1169.
[16] T.C. Lubensky and J. Isaacson, J. Phys. Rev. A20 (1979) 2130.
[17] M. Knezevic and J. Vannimenus, Phys. Rev. B35 (1987) 4988.
[18] S.G. Whittington, G.M. Torrie and D.S. Gaunt, J. Phys. A 16 (1983) 1695.
[19] N. Madras, C.E. Soteros, S.G. Whittington, J.L. Martin, M.F. Sykes, S. Flesia and D.S. Gaunt, J. Phys. A 23 (1990) 5327.
[20] M.F. Sykes, J. Phys. A 19 (1986) 1007.
[21] M.F. Sykes, J. Phys. A 19 (1986) 1027.
[22] M.F. Sykes, J. Phys. A 19 (1986) 2425.
[23] M.F. Sykes, J. Phys. A 19 (1986) 2431.
[24] J.L. Martin, J. Stat. Phys. 58 (1990) 749.
[25] M.F. Sykes, J.W. Essam and D.S. Gaunt, J. Math. Phys. 6 (1965) 283.
[26] D.S. Gaunt, M.F. Sykes, G.M. Torrie and S.G. Whittington, J. Phys. A 15 (1982) 3209.